Title: ***A theoretical investigation of composite overwrapped pressure vessel (COPV) mechanics applied to NASA full scale tests*** Proceedings of the American Society for Composites—Twentieth Technical Conference

Authors: J. C. Thesken
P. L. N. Murthy
S.L. Phoenix
N. Greene
J. Palko
J. Eldridge
J. Sutter
R. Saulsberry
H. Beeson

PAPER DEADLINE: ****JULY 14, 2006****

PAPER LENGTH: ****20 PAGES (Maximum)****

SEND PAPER TO: **Prof. P. K. Mallick**
Professor of Mechanical Engineering
Director of Interdisciplinary Programs
College of Engineering and Computer Science
The University of Michigan-Dearborn
4901 Evergreen Road, 120 MSEL
Dearborn, MI 48128-1491

Tel: (313) 593-5119
Fax: (313) 593-5386
E-mail: ASC2006-papers@umich.edu

NOTE: Sample guidelines are shown with the correct margins. Follow the style from these guidelines for your page format. Pages can be output on a high-grade white bond paper with adherence to the specified margins (8 1/2 x 11 inch paper. Adjust outside margins if using A4 paper). Please number your pages in light pencil or non-photo blue pencil at the bottom.

ABSTRACT

A theoretical investigation of the factors controlling the stress rupture life of the National Aeronautics and Space Agency's (NASA) composite overwrapped pressure vessels (COPVs) continues. Kevlar® fiber overwrapped tanks are of particular concern due to their long usage and the poorly understood stress rupture process in Kevlar® filaments. Existing long term data show that the rupture process is a function of stress, temperature and time. However due to the presence of a load sharing liner, the manufacturing induced residual stresses and the complex mechanical response, the state of actual fiber stress in flight hardware and test articles is not clearly known. This paper is a companion to the experimental investigation reported in [1] and develops a theoretical framework necessary to design full-scale pathfinder experiments and accurately interpret the experimentally observed deformation and failure mechanisms leading up to static burst in COPVs. The fundamental mechanical response of COPVs is described using linear elasticity and thin shell theory and discussed in comparison to existing experimental observations. These comparisons reveal discrepancies between physical data and the current analytical results and suggest that the vessel's residual stress state and the spatial stress distribution as a function of pressure may be completely different from predictions based upon existing linear elastic analyses. The 3D elasticity of transversely isotropic spherical shells demonstrates that an overly compliant transverse stiffness relative to membrane stiffness can account for some of this by shifting a thin shell problem well into the realm of thick shell response. The use of calibration procedures are demonstrated as calibrated thin shell model results and finite element results are shown to be in good agreement with the experimental results. The successes reported here have lead to continuing work with full scale testing of larger NASA COPV hardware.

_____

J. C. Thesken (OAI), P. L. N. Murthy, J. Palko (CRT), J. Eldridge, J. Sutter, NASA- GRC, M.S. 49-7 21000 Brookpark Rd, Cleveland, OH 44135, U.S.A.

S.L. Phoenix, Cornell University, 321 Thurston Hall, Itaca, NY 14853, U.S.A.

N. Greene, R. Saulsberry, H. Beeson, NASA Laboratories Office, NASA Johnson Space Center White Sands Test Facility, P.O. Box 20, Las Cruces, New Mexico, 88004, U.S.A.

INTRODUCTION

The advent of high performance aramid and carbon fiber has enabled the evolution of filament wound pressure vessels capable of extreme energy storage capacity per unit mass, P_BV/W, where P_BV is the product of burst pressure and vessel volume and W is the weight or mass of the vessel. Starting in the 1960's and 70's, this potential was recognized by Johns and Kaufman[2], Lark [3,4] and Faddoul [5] at the NASA Lewis Research Center as a number of design and manufacturing studies began to investigate the technical feasibility of filament wound pressure vessels for space flight. Landes [6] and Ecord [7] published early work describing this technology with reported weight savings of 25 to 30% over comparable all metallic spherical vessels [8]. Today composite overwrapped pressure vessels (COPVs) are essential to numerous NASA power and environmental systems. The majority of older vessel overwraps are made of Kevlar®-49/Epoxy Composites while the newer vessels have Carbon/Epoxy overwraps.

The Kevlar®-49 fiber overwrapped tanks are of particular concern due to their long usage and the poorly understood stress rupture process in Kevlar® filaments. These tanks were designed and developed in the late 1970's and most of them have been in service since delivery in the 1980's. Stress rupture in Kevlar®-49 gives no forewarning so Schmidt and Ecord [9], at the Johnson Space Center, initiated an accelerated stress rupture test program to lead service hardware in actual time at pressure. The occurrence of burst events in that test program motivated the NASA Engineering and Safety Center to establish an Independent Technical Assessment of the COPVs used in NASA applications.

While existing long term data show that the stress rupture process in Kevlar® fiber is a function of fiber stress, temperature and time, it is questionable whether the standard stress – rupture life representation of data may be used by itself for future life extension of NASA COPVs. A substantial contributor to the uncertainty is the presence of load sharing liners and complex manufacturing procedures such that the state of actual fiber stress in flight hardware and sub-scale test articles is not clearly known. As is the case with many ageing aerospace systems, the objective to extend flight certification for this hardware would benefit substantially from two concerted efforts:

1.) Improve the understanding of the component's complex mechanical response, state of stress and deformation.

2.) Improve the fidelity of the stress rupture lifing methods, data base and use of the appropriate reliability framework for the stress rupture threat.

Contributing to the first effort, this paper and a companion paper by Greene et al [1] deal with the theoretical and experimental investigation of the mechanical response of COPVs. The primary focus here and in [1] is the development of a full scale pathfinder test program for vessels in NASA systems. The second effort benefits from a great body of work in the statistical strength theory of fibrous composites and the stress rupture phenomenon that has been developed since the first vessels entered service [10]. The potential improvements for stress rupture lifing methods are highlighted in papers in these proceedings by Phoenix et al[11] and Ledesma-Grimes et al [12]. The former [11] details efforts to enhance the fidelity of the data through the provision of a sound framework for life extension and the latter [12] describes lessons learned in generating stress rupture data. A final paper by Saulsberry et al [13],

concerning NDE methods for COPVs, bridges the two efforts as specialized experimental methods are needed to enhance our ability to understand the mechanical response of COPVs and also offer potential benefits in structural health monitoring/life management activities.

The importance of accurate mechanical response predictions to stress rupture lifing is apparent in how stress rupture life prediction is accomplished. Programs to generate stress rupture data typically comprise a series of short term load to failure tests to determine an 'ultimate strength" for a coupon or test article. This is combined with a group of long term tests where coupons/test articles are held at some constant load until failure occurs. Results of the ultimate strength and long term tests are plotted with the load parameter as a function of time to failure. In addition to Schmidt and Ecords [9] fleet leader test program, the most exhaustive source of available data for the development of Kevlar® fiber lifing models has been the well known Lawrence Livermore National Laboratory (LLNL) data (see e.g. Toland et al [14]).

While the mechanisms of Kevlar® stress rupture remain unclear, Phoenix and Wu [15] show that it has a functional dependency on stress, temperature and time that may be fundamentally linked to the failure process at the fiber bundle level. Scaling this process from small individual filaments to a full scale COPV involves consideration of Weibull size effects [15] in the failure process and understanding of the structural characteristics of each COPV. An excellent overview of statistical strength theory for fibrous composites relevant to stress rupture lifing may be found in Phoenix and Beyerlein [10]. Historically, a ratio of the operating state parameter to the ultimate state parameter has been used to scale life data to dissimilar structures. Lifting parameters such as pressure ratio, stress ratio and percent of ultimate strength are among the common terms used for this comparison. It is important that such parameters be based on the state of the fiber at burst pressure of that vessel. As will be seen, it is difficult to accurately characterize the fiber state at operating and burst pressure levels, in test articles and flight hardware, alike.

An introduction to the mechanical complexities may be found in a review of early COPV design considerations given by Lark [3]; several key points are listed here. It is interesting to note that early designs of high performance COPVs sought to achieve operation fiber stress levels at 60 to 70% of ultimate strength. At these stress levels, strains in the composite exceed the limit for matrix cracking and crazing. As a result, liners were required to achieve viable leak free structures. Early on, elastomers and thin metallic liners were studied carefully due to their potential to achieve the greatest possible energy storage capacity. However, the elastomers examined in early trials were not viable in cryogenic applications and in high pressure gas uses due to cracking and blistering. Thin metallic liners yield during pressurization and must be bonded to the composite overwrap to prevent liner buckling or wrinkling during unloading phases. Lark[3] reported difficulties in achieving leak free liner designs with good fatigue durability in the early attempts to develop COPVs with thin metallic liners. At that time it was suggested that an interim approach to achieve a measure of the improved performance capacity would be to use load bearing liners. This concept was originally suggested by Johns and Kaufman [2] in 1966 and had matured more quickly than the thin metallic liner approach. It is one of the earliest references to the load sharing liner concept which is in use on many NASA systems today. It should be noted that Lark makes a clear distinction between load bearing/load sharing liner designs and the so called thin metallic liner designs. However, the implication that the

load carrying contribution of thin metallic liners is insignificant can lead to false conclusions when deriving the state of stress of such vessels. All of the test article vessels, used in the above named stress rupture programs [9,14], make use of those relatively thin metallic liners with low yield strength. It should be noted that the early published data reduction did not correct for the influence of these thin liners which can introduce significant effects which will be pointed out here and in the papers by Phoenix et al [11] and Grimes-Ledesma et al [12].

Load bearing liners are designed to carry one-third to one-half of the internal pressure load elastically. The remainder of the load is carried by the composite overwrap. After the overwrap is cured in place on the liner an initial proof or sizing pressure is applied which takes the liner beyond its biaxial tensile yield limit and induces a permanent interference pressure between the liner and the overwrap. During unloading the liner transitions from a state of biaxial tension to biaxial compression while the overwrap filaments remain in tension even at zero applied pressure. These locked in residual stresses are superimposed on to the elastic load share of the internal pressure that each element carries. Subsequent operation loads beneath the proof or sizing pressure are carried elastically by both the liner and the overwrap. While analysis indicates that residual stresses contribute over 15% of the composite stress at operating pressures, these values have not been accurately measured and monitored overtime. Recently this important contribution to the fiber stress state was measured using Raman Spectroscopy and fiduciary markers and these results are reported were applicable.

First the fundamental mechanical response of spherical composite overwrapped pressure vessels is described using thin shell theory. Approaches accounting for the influence of elastic-plastic liners and degraded/creeping overwrap properties are reviewed. Graphical representation methods are presented to illustrate the non-linear relationship of applied pressure to Kevlar® fiber stress/strain during manufacturing, operations and burst loadings. These methods may be applied to interpret experimental measurements and to calibrate the model parameters. Examples are given demonstrating the correct calibration of fiber stress as a function of pressure and some comparisons are made to available finite element analyses. Preliminary analysis of the pathfinder tests conducted by the NASA White Sands Test Facility (WSTF)[1] is presented for discussion.

While all of these approaches are of remarkable utility it is important to explore their limitations. Continuing work with the current mechanical analysis finds that it is not fully validated by existing experimental deformation data. Until recently, the state of residual stress at zero pressure remained unsubstantiated by experimental measurement. Moreover, records of internal and external vessel deformation indicate an increased compliance that may not be accurately represented by linear elastic analysis. In addition to the pathfinder vessel testing at WSTF [1], preliminary results of experiments to measure residual stresses are reported. This has pointed to new avenues of investigation exploring the ramifications of non-linear through thickness compressibility and the influence of highly localized plastic instabilities in the liner.

COPV MECHANICS

Theory of Thin Shells

The theory of thin shells is useful to develop a theoretical framework to design and analyze the full scale pathfinder experiments. The following describes the nominal mechanical response of a spherical bi-material pressure vessel. Actual COPV structures will exhibit a non-uniform distribution of stresses and deformation owing to a number of factors. These include the nuances of liner geometry and its interaction with the overwrap winding pattern, the relative stiffness of the liner to the overwrap, the liner-overwrap interface slip characteristics and the presence of incompatible curvature changes. In areas where the liner thickness is uniform, the overwrap may be seen to act as an elastic foundation which cradles the liner. The polar boss areas of liners are typically thickened and more rigid to support the port fixture. The local reinforcement acts as a stiff inclusion in the otherwise uniform metal membrane. In the elastic regime the boss support shields the overwrap from deforming uniformly with the membrane regions of the shell. Liner yielding generally initiates at the transition region between the boss and the membrane areas of the liner. Here plastic strain concentrations are reported up to four times greater than nominal and these are strongly dependent upon nuances of the liner overwrap frictional characteristics. Placed against the natural opening through the winding pattern, the boss acts as a stiff punch against the overwrap once the transition has yielded. Early boss failures were attributed to this stress concentration and new winding patterns increased the amount of fiber in the boss region to better support the boss fixture [3]. The nature of the elastic-plastic behavior of the liner is also prominent in determining the stress state of the overwrap. The liner's plastic deformation and the presence of hardening will affect the sizing process, zero pressure residual stresses, the liners fatigue durability and the overwrap stress state at burst pressure.

With regard to the overwrap, complexity begins in the manufacturing phases with winding parameters, consolidation and curing schedule. The degree of anisotropy of the overwrap is a factor; Gerstle's [16] analysis may be used to demonstrate that high ratios of in-plane to through thickness stiffness can transform a geometrically thin shell into a thick shell problem with significant through thickness gradients. It is also known that filament wound structures can have different hereditary material responses transverse to the fiber depending upon whether the stress is compressive or tensile (Thesken [17]). This non-linearity coupled with the known damage mechanisms associated with the matrix dominated properties of polymer matrix composites make the mechanical response of these COPVs a fundamentally complex problem.

With forethought to the objective of applying a correct lifing parameter for stress rupture, consider the notion of non-uniform fields in the overwrap. Assuming linear elasticity applies, the stress distribution in the composite overwrap may be defined as

$$\sigma_c(\hat{x}, P_c) = f(\hat{x})\sigma_c^n(P_c)$$

(1)

where $f(\hat{x})$ is a form function of the spherical coordinate vector $\hat{x}$ and $\sigma_c^n(P_c)$ is the nominal stress in the overwrap as a function of the composite's pressure load share P_c. The value of the form function at a local maximum of stress is commonly known as a stress concentration factor. Since the distribution function is decoupled from load,

the formation of any stress ratio SR is found to be independent of the spatial distribution function and simplifies to

$$SR = \frac{\sigma_c^o(\hat{x}, P_c^o)}{\sigma_c^B(\hat{x}, P_c^B)} = \frac{\sigma_c^{no}\left(P_c^o\right)}{\sigma_c^{nB}\left(P_c^B\right)} \tag{2}$$

Since the Kevlar®-49 fibers are the dominant load carrying elements of the composite overwrap the notion that the overwrap is linear elastic is a valid first approximation. Additional information from a more detailed linear elastic analysis would provide no further information for a lifing parameter determination. The stress ratio would only change if the spatial distribution function became dependent upon load history i.e. a function of P_c. This is identical to saying that the stress concentration factor at a local maximum is function of load P_c. This would be the case if the composite behaved in a non-linear fashion due to material response or non-linear geometrical effects. Equation (2) has been verified for a bonded liner model of hardware in contracted finite element analysis performed by General Dynamics, Lincoln, Nebraska. Therefore, the use of thin shell theory is the preferred method for characterizing and appraising the performance capability of a COPV.

It should be noted that as presented, this approach to develop a stress ratio is conservative in that the non-linear effects that accelerate fiber stress are more likely to be present at burst. Thus the denominator portion of the stress ratio may be larger than what is predicted in the following thin shell analysis. In the following derivations, the list of variable definitions given in Table I will be utilized for the spherical geometry shown in Figure 1.

TABLE I. VARIABLE DEFINITIONS

Pressure:	P
Inner Wall Radii:	R
Tangential Stress:	σ
Wall thickness:	t
Elastic Modulus:	E
Poisson's ratio:	v
Biaxial modulus:	$E^* = E/(1-v)$
Fiber Volume Fraction:	v_f

Subscript and superscripts:
l –liner; c- composite over wrap, f- fiber ;
y- yield, u – ultimate tensile failure, i – interference load case,
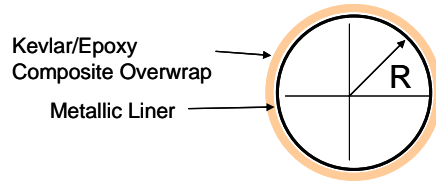P- proof load case, B – burst load case, o –operating load case,
n –nominal

Figure 1. Typical spherical COPV geometry

LOAD EQUILIBRIUM REQUIREMENTS

Load equilibrium in the bi-material COPV vessels requires that the total applied pressure be equal to the sum of the pressure carried by the individual components

$$P = P_l + P_c \qquad (3)$$

For thin shell analysis $R_c \approx R_l >> t_c, t_l, t_f$ where typically the ratio of radii to shell membrane thickness is greater than 10 for all vessels considered here and nominal membrane stress (dropping the n superscript) are

$$\sigma_l = P_l \cdot \frac{R_l}{2 \cdot t_l}$$
$$\sigma_c = P_c \cdot \frac{R_c}{2 \cdot t_c} \qquad (4)$$

It is common to use mid-plane radii for membrane shell theory but comparisons to the exact elasticity solution (see e.g. Roark [18]) show that this over predicts the maximum stress in the shell significantly. Using the inner wall radii in the familiar equations yields a membrane stress that agrees more closely with the maximum stress on the inner wall.

In the case of the quasi-isotropic composite overwrap for a sphere, this formula may be re-written using the fundamental netting assumptions to determine the stress in the fiber as

$$\sigma_f = \frac{\sigma_c}{v_f/2} = \sigma_c \frac{2t_c}{t_f} = P_c \cdot \frac{R_c}{t_f} \qquad (5)$$

From the design stand point it can be said that the ratio of ultimate fiber stress to composite pressure should always meet the following criteria to avoid failure:

$$\frac{\sigma_f^u}{P_c} > \frac{R_c}{t_f} \qquad (6)$$

Characteristics of the liner at yield are also of interest; clearly the pressure load carrying capability of the liner post yield is at least

$$P_l^y = \sigma_l^y \cdot \frac{2t_l}{R_l} \qquad (7)$$

and is only greater if the liner hardens. If the liner is perfectly plastic post yield then the liner load share is constant so the composite load share post liner yield is simply

$$P_c = P - P_l^y \qquad (8)$$

This relation suggests that the burst pressure to fail the overwrap could be predicted by

$$P_B = P_c^u + P_l^y \tag{9}$$

where the composite pressure P_c^u corresponds to the ultimate fiber stress σ_f^u. Conversely the pressure carried by the composite at burst may be defined as

$$P_c^B = P_B - P_l^y \tag{10}$$

and the ratio P_c^B / P_c^u may be seen as a measure of the strength efficiency of the composite overwrap design.

STRAIN CONTINUITY REQUIREMENTS

Continuity of strain and displacement in the liner and composite must be invoked to determine the elastic load sharing prior to proof or sizing of the vessel where the stress in the liner is less than the biaxial yield stress.

$$\varepsilon = \varepsilon_l = \varepsilon_c \tag{11}$$

The biaxial strain for a spherical shell may be written as

$$\varepsilon = \frac{\sigma}{E^*} = P \frac{R}{2tE^*} \tag{12}$$

where the biaxial modulus is E^*.

Insertion into the equilibrium equation relates the applied pressure load to strain as

$$P = P_l + P_c = \left(\frac{2t_l E_l^*}{R_l} + \frac{2t_c E_c^*}{R_c} \right) \cdot \varepsilon \tag{13}$$

The definition of the individual shell stiffnesses as

$$K_l = \frac{2t_l E_l^*}{R_l}$$
$$K_c = \frac{2t_c E_c^*}{R_c} \tag{14}$$

will be used here after.

The composite form of this parameter is the subject of some discussion as different methods have been used to approximate the effective biaxial stiffness. Some design references for the use quasi-isotropic laminate properties such that

$$E_c^* = \frac{E_c^{QI}}{(1 - \nu_c^{QI})} \tag{15}$$

Alternatively the netting analysis approach defines the biaxial modulus as

$$E_c^* = E_f \cdot \nu_f / 2 \tag{16}$$

The elastic load sharing parameters are defined as

$$P_c / P = \frac{K_c}{(K_l + K_c)} = \frac{1}{(K_l / K_c + 1)} = \beta$$
$$P_l / P = \frac{K_l}{(K_l + K_c)} = \frac{1}{(K_c / K_l + 1)} = (1 - \beta) \tag{17}$$

Note that either stiffness ratio (K_l / K_c) or the elastic load sharing parameter β may be used to full specify the designs elastic load share.

PROOF-SIZING AND THE COMPLETE MECHANICAL RESPONSE

The manufacturing process sets final the crucial design parameters that must be evaluated for NASA COPVs. After curing of the composite overwrap, the vessels, is subjected to an autofrettage process or proof-sizing in which an elastic load sharing liner induces a permanent plastic deformation in the liner. After unloading an interface pressure remains that is carried as a tensile preload in the composite and a compression preload in the liner. As the green vessel is loaded to the initial liner yield point, the strains in the vessel are governed by the pressure strain equation (13) up to the liner yield strain where $\varepsilon = \varepsilon_c = \varepsilon_l^y$. At liner yield, the applied pressure P_y that initiates liner yielding is related to the liner yield stress by equations (7) and (17) as

$$P_y = \frac{P_l^y}{(1-\beta)} \tag{18}$$

For a vessel with a perfectly plastic liner that has yielded, the pressure carried by the composite is given by equation (10) so that the strain post yield is given by

$$\varepsilon = \varepsilon_c = \varepsilon_l = \frac{P - P_l^y}{K_c} \text{ where } \varepsilon > \varepsilon_l^y \tag{19}$$

Note that the strain in the vessel during increasing load is controlled by the overwrap which is assumed to remain elastic.

During the unload from proof the liner carries load elastically so the strain in the liner is determined by the total liner strain at proof less the elastic unload strain as

$$\varepsilon_c = \varepsilon_l = \frac{P_P - P_l^y}{K_c} - \frac{P_P - P}{(K_l + K_c)} \tag{20}$$

The residual strain in the overwrap at zero pressure is

$$\varepsilon_c^R = \frac{P_P - P_l^y}{K_c} - \frac{P_P}{(K_l + K_c)} \quad . \tag{21}$$

The interface pressure P_i which the composite and the liner carry identically is found by

$$P_i = P_P - P_l^y - \beta P_P = (1-\beta)P_P - P_l^y \tag{22}$$

Comparing the last two equations it is clear that the residual strain and interface pressure are related by

$$P_i = K_c \varepsilon_c^R \tag{23}$$

All post autofrettage loadings must carry this pressure superimposed on the elastic load share. For the composite overwrap, this is an additive component inducing tensile stress at zero pressure and it is subtractive in the case of the liner inducing compressive stress. Load sharing after proof is governed by the following relations for $P \leq P_P$

$$P_c = \beta P + P_i = (P - P_P)\beta + \left(P_P - P_l^y\right) \tag{24}$$

$$P_l = (1-\beta)P - P_i = (P - P_P)(1-\beta) + P_l^y$$

Deformation history referenced to the initial green state of the vessel is preserved in the strain state of the overwrap so that

$$\varepsilon = \varepsilon_c = \frac{P_c}{K_c} \qquad (25)$$

always gives the strain relative to the newly manufactured vessel. This will not be true if the overwrap exhibits a hereditary response due time and temperature.

Graphical Interpretation and Model Calibration

Figure 2 gives a complete graphical interpretation of the mechanical response of a COPV having a linear elastic overwrap and an elastic-perfectly plastic liner. In this figure, strain is given on the vertical axis and because of continuity, it is identical for the COPV and the individual components. The corresponding pressures and stresses are given on the horizontal axis.

The as-cured vessel in the green state will undergo the sizing operation as depicted by the green lines for the COPV and the liner. Note on the left hand curve for COPV strain – pressure behavior, that when the biaxial yield stress is achieved at a pressure corresponding to P_y, the strain – pressure curve changes slope. Here the changing strain – pressure responses have a common value for strain so

$$\varepsilon = \varepsilon_c = \varepsilon_l = \frac{P_y}{\left(K_l + K_c\right)} = \frac{P_y - P_l^y}{K_c} \qquad (26)$$

providing a graphical way to determine β as

$$\beta = \frac{K_c}{\left(K_l + K_c\right)} = 1 - \frac{P_l^y}{P_y} \qquad (27)$$
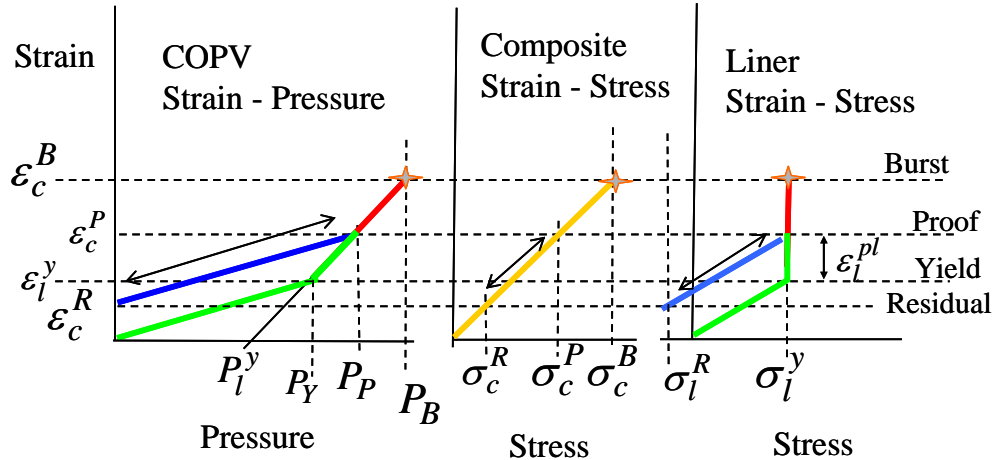

Figure 2. Strain– pressure/stress relationships based on continuity of strain for COPV vessel, composite and liner respectively. Operational loads from $P=0$ to MEOP lie on the blue line for pressures less than P_P

Also, note that the slope of the post yield curve is controlled by the stiffness of the overwrap K_c so that it can be explicitly measured from experimental strain data. The post yield line is offset so that its intercept with the pressure axis corresponds to the pressure carried by the liner at yield P_l^y. This intercept could be converted to the biaxial yield stress of the liner if the liner geometry is known. Note that for a rigid-perfectly plastic liner there would be no strain in the vessel until the stress in the liner reached the yield stress at the applied pressure P_l^y at this intercept point. Thereafter, deformations would be governed by the stiffness of the overwrap and follow the usual post-yield slope. Once the overwrap stiffness K_c is known; it is possible to resolve the stiffness of the liner from a measurement of the pre-yield slopes and solving for K_l.

After the proof pressure is reached, the vessel undergoes elastic unloading. Inspection of the composite and liner strain – stress diagrams shows that both materials exhibit linear elastic response in this regime. The liner has locked in a permanent plastic deformation that will not let it return to zero deformation. At zero applied pressure the composite exhibits a residual tensile stress and the liner exhibits a residual compressive stress. Measurement of the overwrap strain at zero pressure determines residual stresses in the composite and the liner. Equilibrium between the liner and the composite requires that the membrane stress integrated over each thickness must balance the interface pressure.

$$P_i = \sigma_c^R t_c = \varepsilon_c^R E_c^* t_c = -\sigma_l^R t_l \tag{28}$$

Additional constitutive information may be derived from the strain – pressure curves if the geometry of the COPV is well described.

APPLICATION: STRESS RUPTURE TEST ARTICLE

An important example application of the above fundamental principles and graphical analyses is the design appraisal of the test vessels used by Toland et al [14] which comprise the main body of Kevlar fiber stress rupture data. It should be noted that these vessels were designed to operate with the liner above yield stress. In such a case, the pressure carried by the composite at any post yield load point and at burst is given by equations (9,10 and 11) and the fiber stress ratio at these load points is

$$\frac{\sigma_f^o}{\sigma_f^B} = \frac{P_c^o (R/t_f)}{P_c^B (R/t_f)} = \frac{P_c^o}{P_c^B} \tag{29}$$

The stress rupture test data and the design curves have reported the Y-Axis controlled load parameter as a percentage of the composite/fiber strength at burst which is equivalent to multiplying equation (35) by 100% [14]. However, a closer examination of the data indicated that the percentages, plotted, actually correspond to the ratio of the total applied test pressure P_o to the mean static burst pressure P_B of the vessels. As stated in [10]:

"Liner load sharing is nearly negligible. The 1100-0 Al yields at pressures between 24 MPa (3.5 ksi) and 34.5 MPa (5 ksi). (Hydroforming introduces some work hardening, however.) Classical shell formulas indicate that liner yield occurs at an approximate

liner pressure of 1.25 MPa (181 psi). Strain gage data from virgin burst tests graphically illustrate the liner yield."

However the Strain–Pressure curves given in [14] (see Figure 3) do exhibit the distinctive kink indicating the transition of the liner from elastic to plastic response. Analysis of the elastic load sharing parameter for this vessel would predict a severe kink since $\beta = 0.30$ and the composite only carries 30% of the load up to yield. By applying graphical analysis to this strain gage–pressure burst data, it was determined that the pressure carried by the liner at yield is significantly greater than that which had been reported in [14]. Extending a tangent line to the post-yield strain data to the horizontal gives an intercept pressure $P_l^y = 4$ MPa; this corresponds to a yield stress of about 15.9 ksi. This finding prompted tensile testing to be conducted on specimens extracted from a remaining test vessel liner and the yield stress was recorded as 14 ksi.

The combined results indicate that the load carried by the liner is not insignificant. This can be demonstrated graphically by drawing a dashed black line from zero to burst strain point on the strain curve in Figure 3. This line corresponds to a strain – pressure response that is not influenced by the presence of the liner. This line is compared to the red line tangent to the post yield strain data and intercepts the burst point and the pressure P_l^y at zero strain. The offset between these curves indicates that the correct fiber stress ratio for vessels with yielded liners is

$$SR = \frac{P_c}{P_c^B} = \frac{P - P_l^y}{P_B - P_l^y} \tag{30}$$

and values range from 2 to 6% lower than the reported pressure ratios[10]. Pressure ratio and stress ratio are identical at burst pressure and diverge with decreasing applied pressure having the greatest difference at the lowest recorded pressure. The net result is to lower the stress rupture design data base relative to other component operating stress ratios and reduce the perceived reliability margins.[11,12].
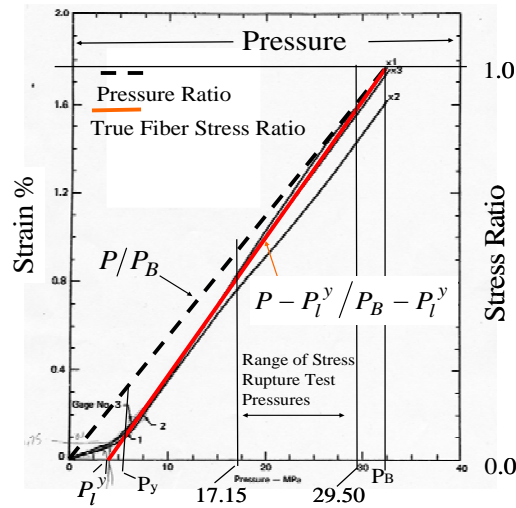

Figure 3. Transformation of strain– pressure relationships into stress ratio calibration curves for the LLNL data base (Figure 6 in Toland et al [14]). Black dashed line is the component pressure ratio and the solid red line is the exact fiber stress ratio.

Vessel Fiber Stress Ratio for Load Sharing Liners

The LLNL vessels described above have significant metallic liners but due to a low yield stress, their contribution to load carrying remains constant in the range where testing took place. Many NASA COPVs have significant liners that carry over 30% of the load. A formulation of a stress ratio for lifing purposes from the thin shell theory can be done using equation (29) where

$$P_c^o = (P_o - P_P)\beta + \left(P_P - P_l^y\right) \tag{31}$$

and

$$P_c^B = P_B - P_l^y \tag{32}$$

Obviously, the pressure – fiber stress conversion term for the numerator and denominator is the same, so the stress ratio is seen to be identical to the composite pressure ratio

$$\frac{\sigma_f^o}{\sigma_f^B} = \frac{P_c^o}{P_c^B} = \frac{(P_o - P_P)\beta + \left(P_P - P_l^y\right)}{P_B - P_l^y} \tag{33}$$

This result is similar to the finding concerning linear elastic stress concentration factors defined in equation (2).

DESIGN AND ANALYSIS OF FULL SCALE PATHFINDER TESTS: PRELIMINARY RESULTS

Background

It is clear from the simple mechanical evaluation of the stress rupture test article used in [14] that correct assumptions about the mechanical response are required to properly utilize the data for lifing purposes. The same is true for the application of stress rupture lifing methods to actual flight hardware. In addition to operating pressure P_o and burst pressure, three parameters are observed to govern the stress ratio in the present formulation in (33): the elastic load sharing factor β, the pressure carried by the liner at yield P_l^y, and the proof-sizing pressure P_P. These three latter parameters may be deduced from analysis or inferred from experiments. Improvements in the accuracy of the theoretical model and/or the governing parameters would be of benefit to the stress rupture lifing process. A number of observations in existing COPV data make it likely that a number of improvements may be possible. First it is noted that external deformation measurements such as the girth displacement measurements plotted against pressure in Figure 4 are considerably lower than predicted by corresponding thin shell theory and finite element analysis.

This may be due to a much stiffer overwrap than currently predicted or due to a thru thickness deformation and stress gradient caused by material anisotropy. The latter proposition is supported by thru thickness measurements made on a vessel at the Johnson Space Center using eddy current measurement techniques in [19]. Calibration of an elastic 3D model to the large thru thickness compression required the transverse modulus to be reduced by a factor of 20. Another observation has been in
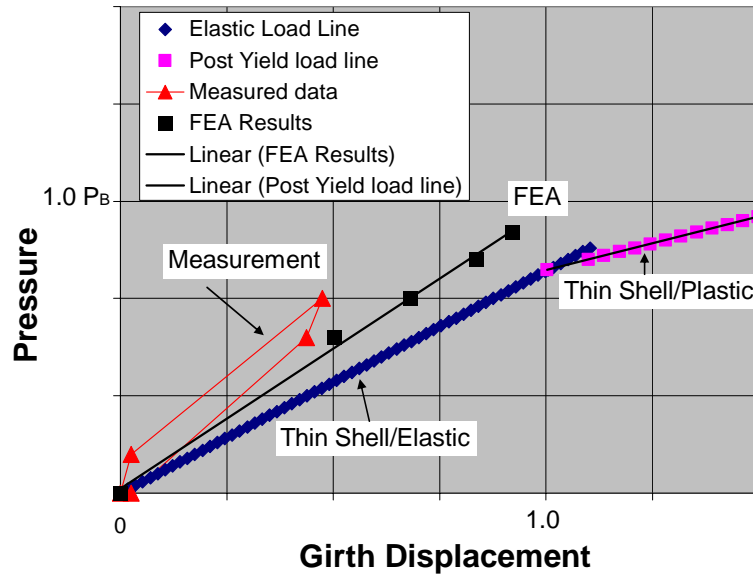
Figure 4. Comparison of actual load-unload pressure – girth displacement data (red curve) to finite element results (cyan blue) and bi-linear thin shell theory (blue-pink curve). Actual vessel girth response measurements appear much stiffer than existing analytical models.

manufacturing records of post-proof internal volume measurements that indicate larger than predicted nominal residual strains. These findings together indicate the need for a series of carefully designed and executed full scale vessel tests to accurately measure the stresses and deformations in the COPVs.

Prior to testing actual hardware, a pathfinder test vessel was chosen to develop the full scale experimental methods and examine the accuracy of the theoretical approach. The pathfinder test article was manufactured by ARDE Inc. and is similar in type to the Kevlar® overwrapped vessel described in [20]. Table 2 provides nominal design parameters for this vessel. Only normalized or qualitative representations of data are given in the following; burst pressure and burst deformations are used as scale factors.

Based on design information provided the girth displacement as a function of pressure has been given in Figure 4. A finite element analysis was conducted using an

TABLE 2 PATHFINDER VESSEL DESIGN PARAMETERS

K_l/K_c	1.067	P_l^y/P_B	0.23
β	0.484	P_i/P_B	0.15
$K_t = K_l + K_c$	$0.917\, P_B/\varepsilon_B$		

ABAQUS model and the resulting total strain distribution as a function of wrap number is given in Figure 5. It is compared to the corresponding thin shell model results for nominal strains in the vessel. The poor agreement between the finite element model and the thin shell theory is believed to be due to the nature of the residual stress distribution in this vessel and the presence of radial gradients thru thickness.

The post sizing proof pressure for this vessel was 0.67 P_B, but based on the room temperature yield stress for the liner and the liner-overwrap inner face pressure, the new yield point may be determined from equation (22) to be 0.73 P_B.

Analysis of Test Data

As described in [1], a series of static load cycles were conducted to 0.67 P_B, 0.87 P_B, 0.93 P_B and burst P_B. Based on the room temperature yield stress for the liner and the residual stress the predicted new yield point is 0.73 P_B. Figure 8 shows the equator strain – pressure response for the first 0.87 P_B cycle to yield the liner. The current yield point (formerly proof pressure) occurs at 0.77 P_B. The total stiffness for the elastic loading portion of the curve is 1.22 P_B / ε_B. The elastic load sharing factor for the composite was found to be 0.514 using equation (27). The corresponding interface pressure is given by equation (22) to be 0.15 P_B. Here again, the actual vessel appears to be 33% stiffer than what is predicted by thin shell theory and the current constitutive model. However, using the graphical analysis of Figure 6, the thin shell model may be calibrated. This has been done and the results are plotted against the strain gage and Raman spectroscopy residual stress measurements for all load cases in Figure 7. The individual strain gages, residual stress measurements and finite element results are plotted as a function of wrap number.

Figure 7 shows strains in the boss area that are low rising to a maximum at wrap 4 and then decreasing only slightly in route to the equator. The relatively homogeneous strain in the membrane region between wrap 5 and 13 supports the notion of using a thin shell model to simulate the observations, but the actual values using the vendor supplied material data does not agree well with the experiments. The calibrated thin shell model using data from the load case of Figure 6 gives reasonable agreement for all load cases. The finite element results match the measured strain distribution quite well except for the comparison to the zero pressure residual stresses measured by Raman spectroscopy. Raman spectroscopy measures elastic strain in the fiber as a spectral shift in scattered light. If the finite element results represent an initial condition based on an elastic response, it is believed that the reduced elastic strains measured by Raman spectroscopy reflect a stress relaxation process that has occurred over the life of the tank. The calibrated thin shell model results agree more closely with the Raman spectroscopy.

The eddy current measurements and the volumetric measurements were crucial to understanding the role of thru thickness gradients in the mechanical performance of COPVs. The volumetric deflections have been paired with external deformation measurements from strain gages and circumferential displacement gages to deduce compressive displacement, Δu_r, of the overwrap. Considering that the overwrap wall is bounded by concentric spherical surfaces, the geometric relationship used to determine compressive displacement is given in the following equation.
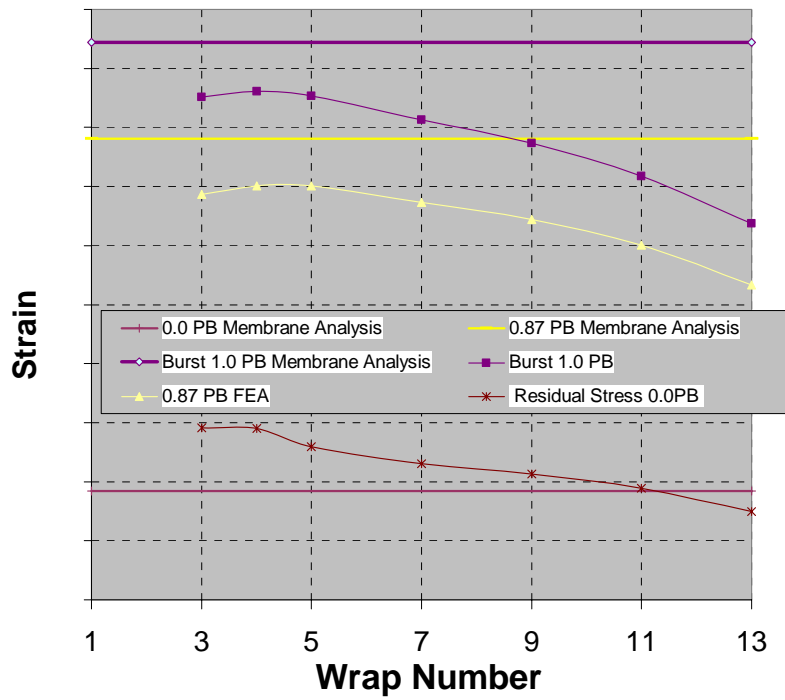
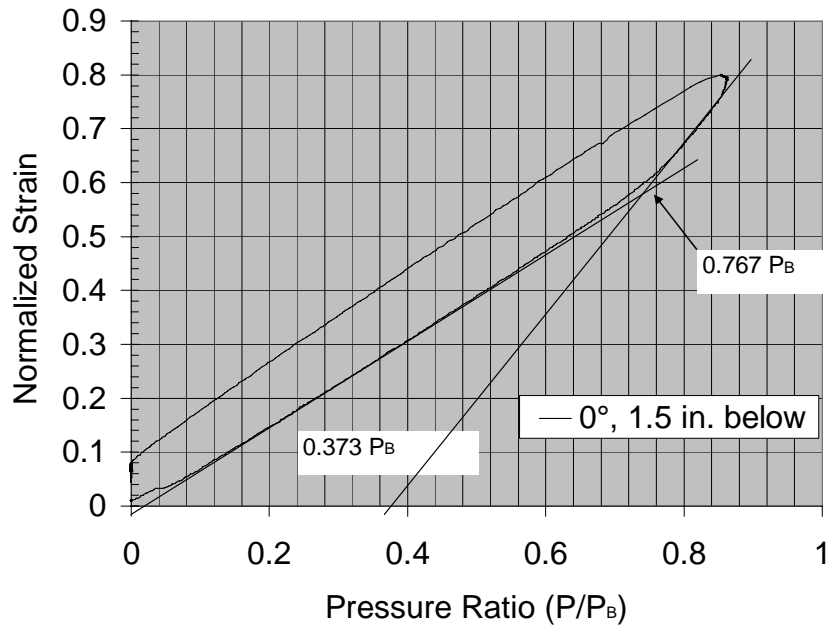Figure 5. Comparison of thin shell model strains to finite element model from boss (wrap 1) to equator (wrap 13)

Figure 6. Normalized equator hoop strain as a function of pressure ratio on first cycle to 0.87 P_B causing liner yielding at 0.767 P_B.
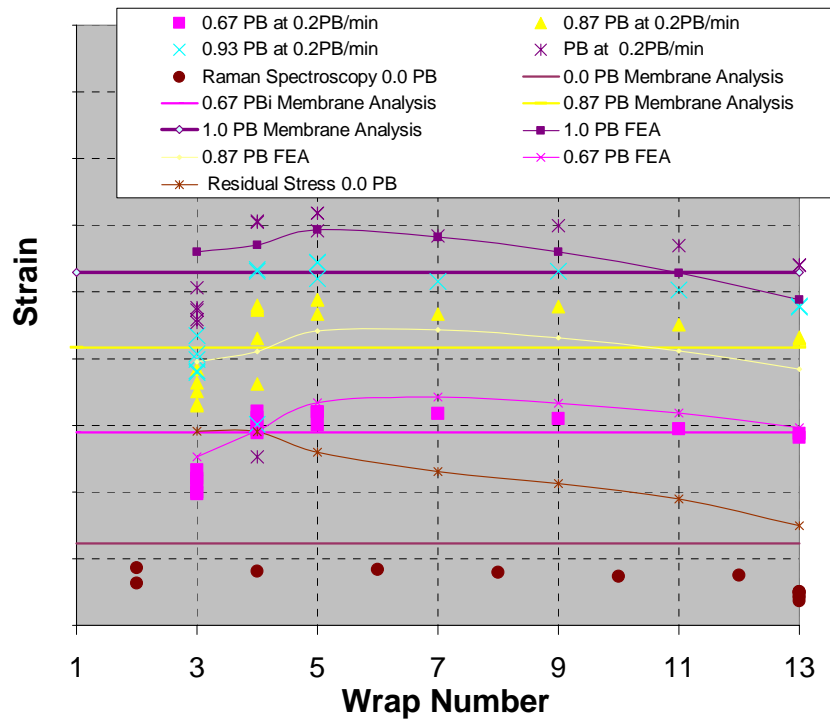
Figure 7. Strain gage measurements and Raman spectroscopy residual strain measurements as a function of wrap number 1 (boss) to the 13 (equator) compared to the calibrated thin shell theory (horizontal lines) and the finite element analysis.

$$\Delta u_r = \left(\varepsilon_{outer} \cdot r_{outer}\right) - \left(\varepsilon_{inner} \cdot r_{inner}\right) \tag{34}$$

where the inner strain is deduced from the vessel volume change and the outer strain is from the selected external measurement device.

The compressive displacements are given as a function of pressure ratio and are compared to the eddy current sensor and the finite element results in Figure 8. All data has been normalized relative to the compressive displacement at burst given by the finite element analysis. Depending on sensor location, the displacements measured by eddy current are of the same order to about 1.5 times greater than those extracted from the finite element analysis. The analysis using volumetric deformation and surface deformations finds values up to 5 times larger than those in the finite element analysis. The discrepancy between the eddy current measurements is currently being evaluated. It is suspected that the bonded on eddy current gages may be lifting away from the outer surface as the load is applied. This would be true if edge cracks from the bond line propagated under the sensor as the Kevlar substrate is loaded. In any case, the findings support the general proposition that thru thickness gradients may play a very significant role in determining the stress and strain state that controls stress rupture failure and burst due to monotonic overload.
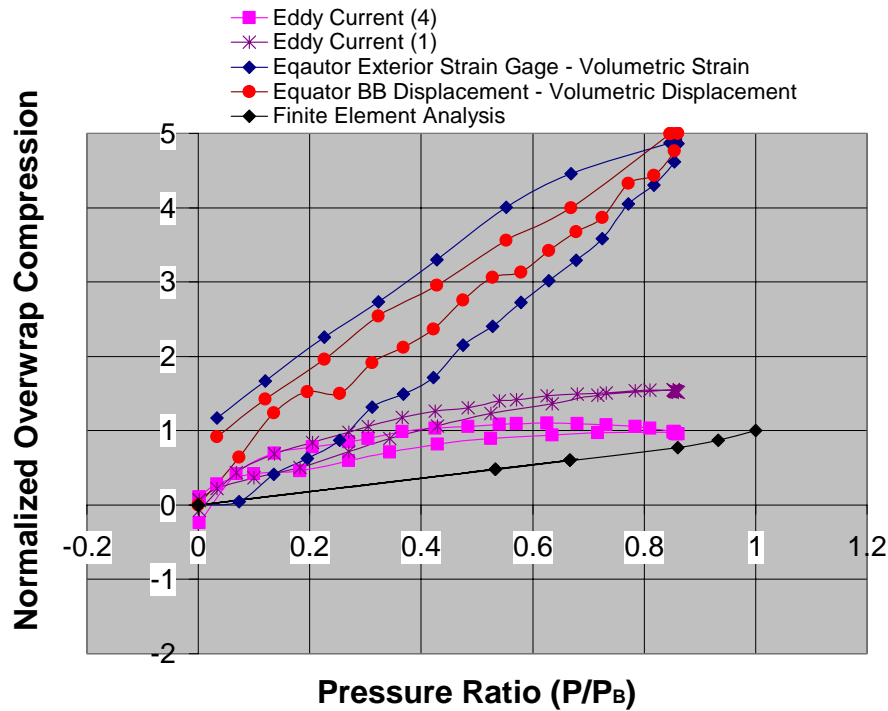
Figure 8. Thru thickness non-dimensional compressive displacement of the composite overwrap as a function of the applied pressure ratio.

CONCLUSIONS AND CONTINUING WORK

This paper describes an effort to better understand the mechanical response, stress and deformation state in Kevlar® overwrapped pressure vessels. The purpose of the work is to enhance the accuracy of stress rupture life prediction and reliability methods applied to NASA COPVs. The focus in this case has been the development and application of methods to design and analyze the full scale pathfinder tests described here and in [1].

A review consisting of early design approaches considered leading to the load sharing liner concepts in use on many NASA systems, has been given. Despite the complexity of COPVs, thin shell theory has been shown to capture the nominal mechanical response of COPVs and is readily amenable to direct calibration from experiments. Strain gage measurements and finite element results showed rather large regions of the COPV where nominal response was obtained. While the actual features of the mechanical response are identifiable, eg bi-linear deformation response showing the liner yield point, accurate quantitative results seems to require calibration of the model parameters. Examination of the thru thickness compressive deformations of the overwrap suggests that the overwrap behaves more as a thick shell. This is not surprising as Phoenix and Skelton [21] provided experimental evidence that the transverse modulus of Kevlar was much lower than that previously reported in the manufacturer's data. Residual stress distributions determined by Raman spectroscopy were quite low in comparison to finite element analysis results indicating that stress

relaxation may be reducing the zero pressure stress state. This relaxation process may likely be strongly coupled to the transverse response of the overwrap.

Based on the success of the pathfinder tests and analysis described here and in [1], work continues on the full scale tests of the largest NASA COPVs at WSTF. In addition, methods to harvest and test strand specimens from overwraps have recently been developed and tested. Preliminary transverse compression tests have also been conducted and microscopic examination of the overwrap and the liner materials is underway. The objective is to have the mechanical response for a number of important NASA COPVs fully characterized within the year.

REFERENCES

1. Greene N. et al "Experimental Investigation of NASA Composite Overwrapped Pressure Vessels for Stress Rupture Life"to appear The 21st Annual Technical Conference of the American Society for Composites, Dearborn, MI, 2006.
2. Johns, R. H. and A. Kaufman. 1966. Filament-Overwrapped Metallic Cylindrical Pressure Vessels, in AIAA/ASME Seventh Structures and Materials Conference, AIAA, 52-63.
3. Lark, R.F. 1973. "Filament-wound Composite Vessel Materials Technology", NASA TMX – 68196,.
4. Lark, R.F., 1977. "Recent Advances in Lightweight, Filament-wound Composite Pressure Vessel Technology", NASA TM 73699,
5. Faddoul, J. R. "Structural Considerations in Design of Lightweight Glass –Fiber Composite Pressure Vessels", in Proceedings of the Second International Conference on Pressure Vessel Technology. Part I – Design and Analysis, ASME, 561-572, 1973.
6. Landes, R. E. 1973 "Glass Fiber Reinforced Metal Pressure Vessel Design Guide", NASA CR-120917, Structural Composites Industries, Inc.
7. Ecord, G. M. "Filament wound pressure vessels with load sharing liners for Space Shuttle Orbiter applications" National Symposium and Exhibition on Bicentennial of Materials Progress, Los Angeles, CA, April 6-8, 1976 , JAN 1, 1976
8. Landes, R. E. 1976. "Filament –Reinforced Metal Composite Pressure Vessel Evaluation and Performance Demonstration" Structural Composites Industries, Inc. Report SCI-75154, also NASA CR-134975
9. Schmidt, W. W. and Ecord, G. M "Static fatigue life of Kevlar® aramid/epoxy pressure vessels at room and elevated temperatures", AIAA PAPER 83-1328 ; Jun 1, 1983
10. Phoenix S.L. and I. J Beyerlein. 2000. *Chapter 1.19 Statistical Strength Theory for Fibrous Composite Materials*. COMPREHENSIVE COMPOSITE MATERIALS Ed A. Kelly, C. Zweben, PERGAMON
11. Phoenix S.L et al "Reliability Modeling of the Stress-Rupture Performance of Kevlar® 49/Epoxy Pressure Vessels: Revisiting a Large Body Stress Rupture Data to Develop New Insights" to appear in The 21st Annual Technical Conference of the American Society for Composites, Dearborn, MI, 2006.
12. Grimes-Ledesma, L. et al "Testing and Analysis of Carbon Fiber Composite Overwrapped Pressure Vessel Stress Rupture Lifetime" to appear in The 21st Annual Technical Conference of the American Society for Composites, Dearborn, MI 2006
13. Saulsberry, R. et al "Nondestructive Methods Supporting NASA Composite Overwrapped Pressure Vessel Assessment" The 21st Annual Technical Conference of the American Society for Composites, Dearborn, MI, 2006.
14. Toland, H., et al., March 31,.1978 "Stress Rupture Life of Kevlar®/Epoxy Overwrapped Pressure Vessels", LLNL Report # UCID-17755, Livermore, California
15. Phoenix, S. L., and Wu, E.M., "Statistics for The Time Dependent Failure of Kevlar®-49/Epoxy Composites: Micromechanical Modeling and Data Interpretation." IUTAM Symposium on Mechanics of Composite Materials, Pergamon. 1983.

16. Gerstle, F.P. Jr., "Analysis of Filament-Reinforced Spherical Pressure Vessels", ASME STP 546, 604-631, 1974.
17. Thesken, J.C. et al "Time Temperature Dependent Response of Filament Wound Composites for Flywheel Rotors" Composite materials: Testing and Design Fourteenth Volume, ASTM STP 1436. C. E. Bakis,Ed. ASTM International, West Conshohocken, PA, 2003.
18. Roark, R. J. and W. C Young,. 1975 Formulas for Stress and Strain, fith edition, McGraw-Hill Inc.
19. C. J. Wesselski (1977) NASA MPS Pressure Vessel Test Structures Branch Report Johnson Space Center, January 1977. .
20. Escalona, A   "Design of a high performance load sharing lined COPV for ATLAS/Centaur" AIAA-1997-3031 AIAA/ASME/SAE/ASEE Joint Propulsion Conference and Exhibit, 33rd, Seattle, WA, July 6-9, 1997.
21. Phoenix S. L and J. Skelton. 1974. "Transverse Compressive Moduli and Yield Behavior of Some Orthotropic, High-Modulus Filaments", *Textile Research Journal* Vol. 44, No. 12, December